An immersed boundaryregularised Lattice Boltzmann Method for acoustic simulations of FSI problems

Author:
Rajamuni, Methma; Liu, Zhengliang; Tian, Fangbao; Lai, Joseph; Young, John; Ravi, Sridhar

An immersed boundary-regularised lattice Boltzmann method for acoustic simulations of FSI problems

Methma M Rajamuni[1][*], **Zhengliang Liu**[2], **Sridhar Ravi**[1], **Fang-Bao Tain**[1], **John Young**[1] and **Joseph Lai**[1]

[1] University of New South Wales Canberra, ACT 2610, Australia
[2] Southern University of Science and Technology, Shengzhen China 518055
[*]mailto: methma.mm@gmail.com

Abstract

Fluid-structure acoustic interaction problems are becoming more popular with the recent development of computational techniques. This work focuses on developing and validating an efficient numerical method to examine aeroacoustic in fluid-structure interaction problems, such as the noise of flapping insect wings or vortex-induced vibration of a bluff body. Capturing acoustic waves in a numerical simulation through the pressure field fluctuations is challenging, as a large spatial domain with high resolution and extremely small time step are generally required in aeroacoustic simulations. Thus, selecting an appropriate methodology is critical in aeroacoustic simulations. Here, the efficient lattice Boltzmann method (LBM), which describes the evolution of mesoscale velocity distribution functions, based on free-streaming and collision is used. The fluid-solid interface is modelled using the well-established immersed boundary method. There are many different versions of LBM with distinct collision operators. The recursive and regularized Bhatnagar-Gross-Krook (RR-BGK) collision operator, which was developed based on higher-order Hermite polynomials, was used to improve the numerical stability and accuracy. At the outer boundary of the domain, a non-reflective boundary condition was employed to overcome the reflections of sound waves. Two benchmark cases: flow past a stationary sphere and sound generated by the flapping wings of an insect in hovering flight, were conducted as validation studies. Results obtained by the immersed boundary-regularised LBM showed good agreement with numerical simulations in the literature, demonstrating the capability of capturing moving boundaries and acoustic propagation.

1   Introduction

The development of computational technologies allows us to examine complex fluid-structure interactions having subtle nature. Noise generation in the flapping motion of an insect wing and the flow-induced vibration of a flag pole are examples of fluid-structure acoustic interaction problems. It is interesting to know how big birds like owls and eagles can generate a high lift and thrust to manoeuvre in the sky by maintaining a silent flight. If the mechanism of noise mitigation in bird's flight is understood then this knowledge could be used to reduce the annoying noise generated by several man-made objects, such as unmanned aerial vehicles, helicopters and wind turbine blades. Although it is an fascinating research topic, only a little research have focused on aeroacoustic. This is mainly due to the complexity of setting up such a problem experimentally or computationally. Hence, the focus of this article is on developing an efficient numerical method to examine aero-acoustics in fluid-structure interaction (FSI) problems, as an initial work.

Capturing subtle pressure fluctuations due to acoustic waves in a numerical simulation is challenging. A heavy spatial domain with high resolution is required together with an extremely small time step to capture these soft-acoustic signals in computational aeroacoustic simulations Tam (2004).

Therefore, it is challenging to simulate acoustics problems using the conventional methods of solving Navier-Stocks equations, as higher-order accuracy, low-dispersion and low-dissipation spatial discretisation and time marching schemes are necessary Shao and Li (2019). Nevertheless, the lattice Boltzmann method (LBM), that describes the evolution of mesoscale velocity distribution functions, based on the free-streaming and collision is intrinsically suitable for aeroacoustic simulations. The simple nature of the LBM, efficiency with parallel simulations, small-time steps than in the NS method, and large spatial resolutions make LBM more attractive for acoustic simulations Brogi et al. (2018); Sharma et al. (2020). Hence, LBM was chosen to model the fluid in this study. It is also crucial to select a suitable model for the collision operator. The recursive and regularized BGK collision model is used, as it was found more suitable for acoustic simulations Brogi et al. (2017).

In the context of LBM, the most popular methods of modelling the fluid-structure interface of FSI problems are the bounce-back methods and immersed boundary methods. With rigorous analysis, Chen et al. (2014) revealed that the immersed boundary methods are more appropriate for moving boundary problems as they produce less disturbing spurious pressure waves. Moreover, Cai et al. (2018) validated the capabilities of immersed boundary lattice Boltzmann method of acoustic simulations. Immersed boundary methods are widely used to solve a variety of flow problems, as they are computationally efficient and suitable to handle moving and deforming boundaries Roy et al. (2020). Therefore, a widely used diffusive interface immersed boundary method integrated with the lattice Boltzmann method, which is known as IBLBM, was chosen for this study.

In computational studies, a truncated domain is used, even in the simulations of open boundary problems, like flapping insect wings. Although this can be easily rectified by a correct choice of boundary condition for non-acoustic simulations, special techniques are required in acoustic simulations to avoid non-physical acoustic wave reflections from the boundaries to the computational domain. Characteristics boundary conditions and absorbing boundary conditions are two widely used non-reflective boundary condition approaches. Testing six different non-reflective boundary conditions Kam et al. (2007) found that the overall performance of the absorbing boundary layer condition was the best. In the framework of LBM, Shao and Li (2019) claimed that absorbing boundary layer conditions have better non-reflective performances than characteristic boundary conditions. In the absorbing boundary conditions, a layer of nodes/cells is added to the domain to absorb the sound waves before they reach the outer boundary. The perfectly match layer (PML) condition is the most popular absorbing boundary layer approach. As the name implies, the governing equations of the added layer match perfectly with the fluid domain at the interface Najafi-Yazdi and Mongeau (2012). Consequently, this method produces the minimal reflection of sound waves from the fluid and absorbing layer interface. Thus, PML was used to avoid the non-physical sound wave reflections.

The work presented in the paper is the initial work of developing an efficient and stable numerical method to examine complex fluid-structure acoustic interaction problems. The structure of the paper is as follows: next, section 2 describes the numerical methods developed in detail; then, section 3 presents a couple of validation studies to show the capabilities of the numerical method; finally concluding remarks are given in section 4.

2 Numerical Methodology

This section presents the numerical methods developed to solve complex fluid-structure-acoustic interaction problems. The lattice Boltzmann method is used to model the fluid. Since LBM is based on the evolution of mesoscale velocity distribution function, $f = f(\boldsymbol{x}, \xi, t)$, it can be directly used to observe acoustics waves without solving an additional equation. Thus, it's far more efficient than the conventional methods of solving Navier-Stokes equations. The LBM is based on solving the simple lattice Boltzmann equation

$$\frac{\partial f}{\partial t} + \xi_\alpha \frac{\partial f}{\partial x_\alpha} + \frac{S_\alpha}{\rho} \frac{\partial f}{\partial \xi_\alpha} = \Omega(f), \tag{1}$$

where ρ is the density, ξ is the particle velocity, S is the body force, Ω is the collision operator, and $\alpha \in \{x, y, z\}$. The simple and vastly used Bhatnagar-Gross-Krook or BGK collision operator,

$$\Omega = -\frac{1}{\tau}(f - f^{eq}), \tag{2}$$

relaxes f towards the local d-dimensional equilibrium, $f^{eq} = \frac{\rho}{(2\pi)^{(d/2)}} e^{-\frac{(\xi-u)^2}{2}}$, at a rate determined by the relaxation time, τ. Here $\boldsymbol{u}$ is the fluid velocity.

Using the Hermite series, the velocity distribution function can be expand as

$$f(\boldsymbol{x}, \boldsymbol{\xi}, t) = \omega(\boldsymbol{\xi}) \sum_{n=0}^{\infty} \frac{1}{n!} \boldsymbol{a}^{(n)}(\boldsymbol{x}, t) : \boldsymbol{H}^{(n)}(\boldsymbol{\xi}), \tag{3}$$

where $\omega()$ is the weight function, $\boldsymbol{H}^{(n)}$ and $\boldsymbol{a}^{(n)}$ are the nth order Hermite polynomials and their coefficients in d-dimensions, respectively and ":" denotes the full contraction. The Hermite polynomial coefficients are calculated by

$$\boldsymbol{a}^{(n)}(\boldsymbol{x}, t) = \int f(\boldsymbol{x}, \boldsymbol{\xi}, t) \boldsymbol{H}^{(n)} d^d \xi. \tag{4}$$

In LBM, the velocity space, $\boldsymbol{\xi}$, is discretised using the Gauss-Hermite Quadrature rule, and the velocity sets used for 2D and 3D simulations are D2Q9 and D3Q19, respectively.

The standard LBM is developed by descritizing f^{eq} using Hermite polynomials upto 2nd order, as it is sufficient to reproduce the relevant physics. Nevertheless, the recursive and regularized BGK collision operator introduced by Malaspinas (2015) with higher order terms is used for this study. Brogi et al. (2017) showed that it is more suitable for acoustic simulations, as it improves the stability.

2.1   Recursive and Regularized Lattice Boltzmann Method

The full derivation process of the recursive and regularized collision operator was detailed in Malaspinas (2015), and only a brief description is given here. In this collision operator, both equilibrium and non-equilibrium components of the distribution function are considered, i.e., $f = f^{eq} + f^{neq}$ (Coreixas et al., 2017). The equilibrium and non-equilibrium distribution functions can be expand with the Hermite series with coefficients $\boldsymbol{a}^{(n), eq}$ and $\boldsymbol{a}^{(n), neq}$, respectively. Although, $\boldsymbol{a}^{(n), neq}$ vanishes for $n = 0$ and 1, it is non-zero for $n \geq 2$.

In this study, we used Hermite series terms up to 4th order to improve the accuracy and stability. By considering the recursive and orthogonal properties of Hermite polynomials only some of the higher-order terms are used to obtain f_i^{eq} and f_i^{neq}, here i is the velocity direction. For the D2Q9 model of 2D simulations, they are as follows:

$$f_i^{eq} \approx \omega_i \left(\rho + \frac{\boldsymbol{a}^{(1),eq} : \boldsymbol{H}^{(1)}}{c_s^2} + \frac{\boldsymbol{a}^{(2),eq} : \boldsymbol{H}^{(2)}}{2c_s^4} + \frac{\rho \left(u_x^2 u_y H_{i,xxy}^{(3)} + u_x u_y^2 H_{i,xyy}^{(3)} \right)}{2c_s^6} + \frac{\rho \, u_x^2 u_y^2 H_{i,xxyy}^{(4)}}{4c_s^8} \right), \tag{5}$$

$$f_i^{neq} \approx \omega_i \left(\frac{\boldsymbol{a}^{(2),neq} : \boldsymbol{H}^{(2)}}{2c_s^4} + \frac{\left(a_{xxy}^{(3),neq} H_{i,xxy}^{(3)} + a_{xyy}^{(3),neq} H_{i,xyy}^{(3)} \right)}{2c_s^6} + \frac{a_{xxyy}^{(4),neq} H_{i,xxyy}^{(4)}}{4c_s^8} \right). \tag{6}$$

The computation of $\boldsymbol{a}^{(n),eq}$ can be linked to the hydrodynamics moments of the velocity field. The elements of coefficients $\boldsymbol{a}^{(2),neq}$ are approximated by taking the second moment of $f_i - f_i^{eq}$, i.e., $a_{\alpha\beta}^{(2),neq} \approx \sum_i \xi_\alpha \xi_\beta (f_i - f_i^{eq})$ for $\alpha, \beta \in \{x, y, z\}$. The elements of $\boldsymbol{a}^{(3),neq}$ and $\boldsymbol{a}^{(4),neq}$ can be obtained using the recursive property, see Coreixas et al. (2017) for more information. The body force term $\frac{S_\alpha}{\rho} \frac{\partial f}{\partial \xi_\alpha}$ in equation 1 is decomposed into the ith velocity direction using the Hermite expansion of 4th order by

$$S_i(x,t) \approx \omega_i S_\alpha \left(H_\alpha^{(1)} + u_\beta H_{\alpha\beta}^{(2)} + \frac{1}{2} u_\beta u_\gamma H_{\alpha\beta\gamma}^{(3)} + \frac{1}{6} u_\beta u_\gamma u_\delta H_{\alpha\beta\gamma\delta}^{(4)} \right). \tag{7}$$

A second-order accurate discretization scheme is derived by changing variables; $\bar{f}_i = f_i - (\Omega_i + S_i)/2$, $\bar{f}_i^{neq} = \bar{f}_i - f_i^{eq} + S_i \Delta t/2$, and $\bar{\tau} = (2\tau + \Delta t)/(2\Delta t)$ to solve the lattice Boltzmann equation as

$$\bar{f}_i(x + \xi_i \Delta t, t + \Delta t) = f_i^{eq}(x,t) + \left(1 - \frac{1}{\bar{\tau}} \right) \bar{f}_i^{neq}(x,t) + \frac{\Delta t}{2} S_i(x,t). \tag{8}$$

This equation is solved in two steps: *collision step* computes the right-hand side of the equation and *streaming step* streams the collided distribution function to neighbouring nodes according to the velocity model used.

2.2 Diffusive Immersed Boundary Method

Immersed boundary methods are widely used in numerical studies to handle the fluid-structure interface with a non-deforming grid. These methods were developed with *Eularian* and *Lagrangian* systems representing the fluid and the fluid-structure interface, respectively. As the interface is immersed in the fluid, it needs to satisfy two conditions to have a continuous governing equation: 1. the velocity of the interface should match the velocity of the surrounding fluid and 2. the momentum exchange between the interface and fluid should match. For the fluid to be aware of the presence of the fluid-structure boundary, the body force term, $S(x,t)$, is added to the LB equation.

As we wish to consider complex geometries in future, like flexible wings of birds, the simple diffusive interface method is considered with an iterative algorithm to couple the Eulerian and Lagrangian systems. Our iterative penalty force algorithm is similar to the multi-direct forcing algorithm of Kang and Hassan (2011). The only difference is we calculate the Lagrangian force density by $F_L = \alpha^*((\boldsymbol{u}_B - \boldsymbol{u}_L)$, while they computed it using $F_L = 2\rho((\boldsymbol{u}_B - \boldsymbol{u}_L)/\Delta t$, where $\boldsymbol{u}_B$ and $\boldsymbol{u}_L$ are the desired and calculated velocity of the boundary, respectively, and $\alpha^* = 30$.

2.3 PML Condition to Minimize Acoustic Reflections

The perfectly matched layer condition is used to minimize the acoustic wave reflection into the domain from the outer boundaries. It is an absorbing boundary condition in which a layer of nodes is added outside of the interior fluid domain to absorb acoustic waves as they travel through this region. PML condition is developed based on the evolution of a linear hyperbolic system, where waves decay exponentially within the PML without reflection from the PML/interior domain interface. Najafi-Yazdi and Mongeau (2012) implemented it in the framework of LBM as an additional collision term, Ω_{PML} determined for 2D simulations by

$$\Omega_{PML} = -\sigma(2\tilde{f}^{eq} + \sigma Q + \xi \cdot \nabla Q), \tag{9}$$

whre σ is the dampling coefficient, $\tilde{f}^{eq} = f^{eq} - \bar{f}^{eq}$ and $\bar{f}^{eq}$ are the pertub and mean components of f^{eq}, and $\frac{\partial Q}{\partial t} = \tilde{f}^{eq}$. The damping coeffecent is related to the distance from the current node to the open
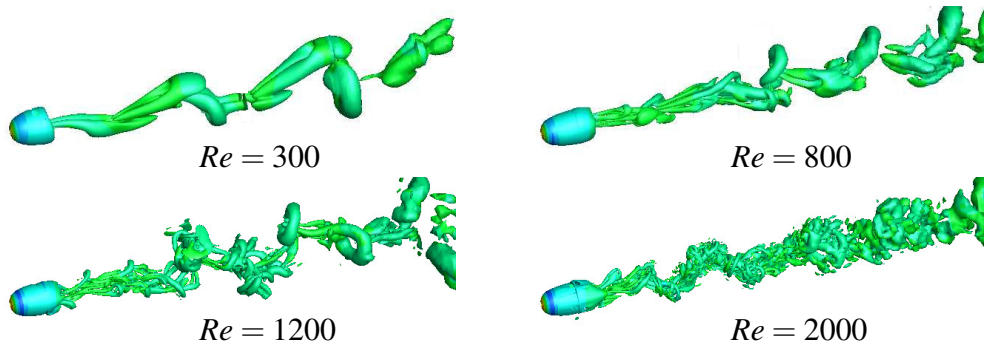
Figure 1. Visualization of the wake of flow past a sphere at $Re = 300$, 800, 1200 and 2000.

Study	$Re = 300$			$Re = 500$		
	$\overline{C}_D$	$\overline{C}_L$	St	$\overline{C}_D$	$\overline{C}_L$	St–2
Present	0.657	0.092	0.140	0.552	0.064	0.189
Kim et al. (2001)	0.657	0.067	0.137	-	-	-
Johnson and Patel (1999)	0.656	0.069	0.137	-	-	-
Poon et al. (2014)	-	-	-	0.56	0.05	0.15
Rajamuni (2018)	-	-	-	0.57	0.06	0.18

Table 1. Comparison of computed time-averaged drag coefficient, $\overline{C}_D$, time-averaged lift coefficient, $\overline{C}_D$, and Strouhal number, St, of flow past a stationary sphere.

boundary in the PML region as $\sigma = \sigma_{max} \, n^2 / n^2_{max}$, where $\sigma_{max} = 0.06$, n is the minimal distance from the current node to the outer-boundary, and $n_{max} = 120$ is the width of the PML region.

3   Validation Studies

This section presents two validation studies to show the capabilities of $2D$ and $3D$ solvers developed for fluid-structure interaction problems.

### 3.1   Validation Study 1: Flow Past a Stationary Sphere

To check the performances of the $3D$ solver developed, we studied flow past a stationary sphere for the Reynolds numbers range $100 \leq Re \leq 2000$. As found in the literature, the flow was steady at $Re = 100$ and 250 and unsteady with hairpin loop vortex shedding for $Re \geq 300$. Figure 1 illustrates the visualisation of the wake behind the sphere. As can be seen, the vortex shedding was axisymmetric at $Re = 300$, irregular at 800, and chaotic at 1200 and 2000. This agrees well with the findings of the literature. Table 1 compares the calculated time-averaged drag and lift coefficients, $\overline{C}_D$ and $\overline{C}_L$ respectively, and the Strouhal number, St. Our predictions match well with the literature for both $Re = 300$ and 500. Many studies reported that $\overline{C}_D \approx 0.46$ at $Re = 1000$. We found that $\overline{C}_D$ decreased from 0.48 to 0.44 with the increment of Re from 800 to 1200. All these results validate the capabilities of the solver of $3D$ flow simulations.
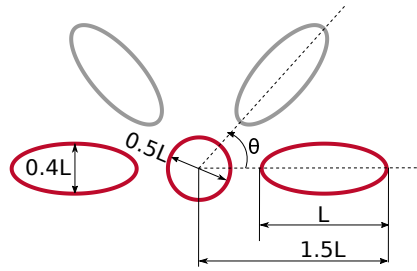
Figure 2. Schematic of the modelled flapping motion. The circle in the middle represents the centre body, while the two ellipses represent two wings.
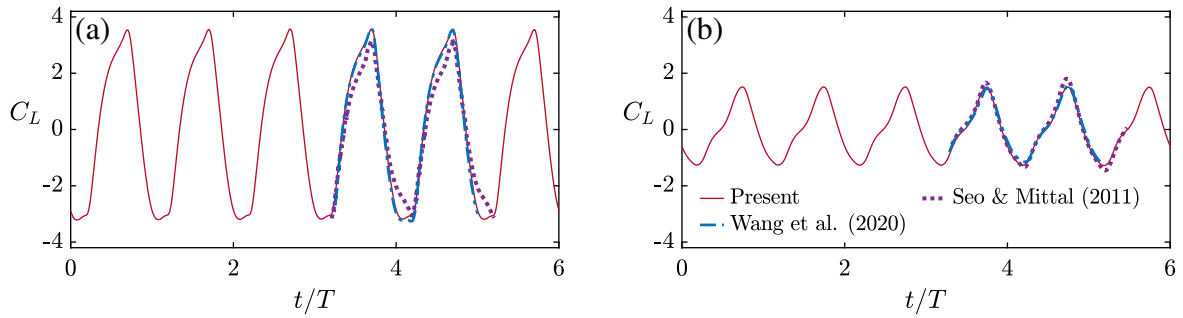
Figure 3. Comparison of the time variation of the lift force coefficient, C_L at (a) a wing and (b) centre body with the literature. Our results match well with the findings of Seo and Mittal (2011) and Wang et al. (2020).
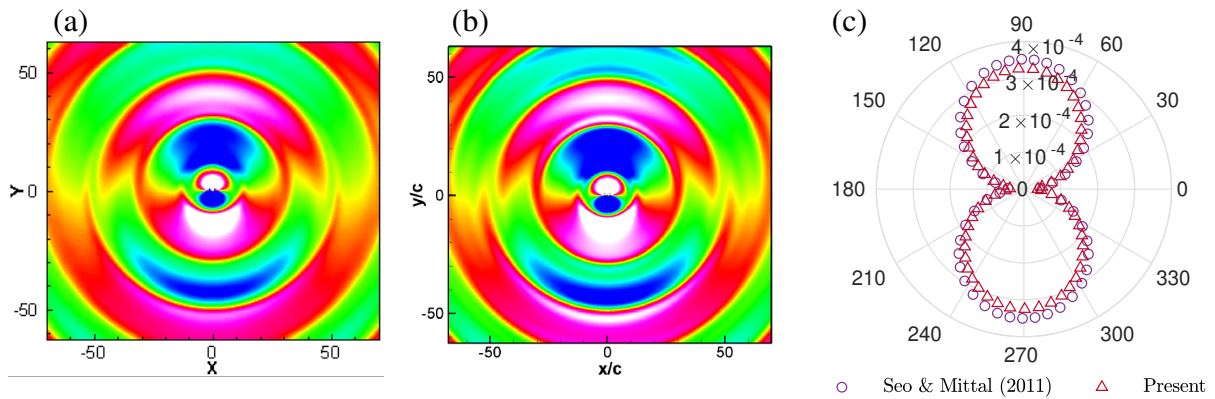
Figure 4. Comparison of the acoustic field generated by the modelled flapping motion: (a) current prediction and (b) findings of Seo and Mittal (2011) of the instantaneous acoustic field, and (c) comparison of the root-mean-square of fluctuating pressure measured at a distance of 50L.
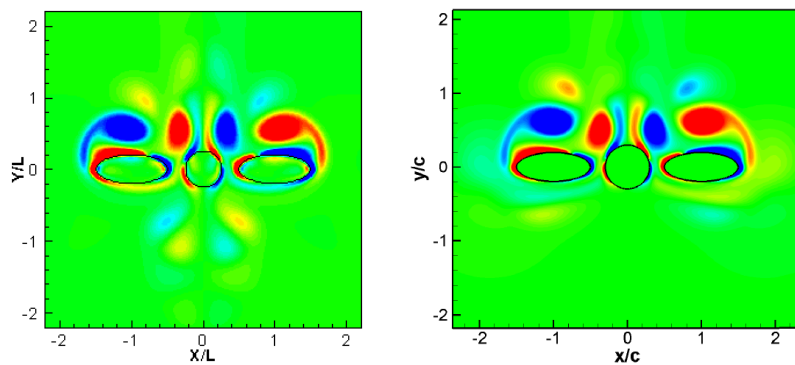
Figure 5. Instantanious vorticity contuors: (a) Present and (b) Seo and Mittal (2011).

3.2 Validation Study 2: Sound Generated by a Flapping Motion

To validate the capabilities of the solver in handling moving boundaries and acoustic, an insect in hovering flight is considered. A simple $2D$ geometry of a circle and two ellipses was used to represent the centre body and two wings of the insect, see figure 2 for the schematic of the setup. The two wings flap symmetrically, and the flapping motion of the wings is prescribed by

$$\dot{\theta} = \frac{U_{max}}{r_{tip}} sin\left(\frac{2\pi t}{T}\right), \tag{10}$$

where U_{max} is the maximum wing tip velocity at $r_{tip} = 1.5L$, L is the length of the wing, and T is the flapping period. The Reynolds number is set to 200, the Mach number based on U_{max} is fixed at 0.1, and the Strouhal number is set to $L/TU_{max} = 0.25$. A computational domain of $326.4L \times 326.4L$ is used for the simulation with six multi-block grid refinements leading to the smallest grid spacing of $0.02L$. This grid consists of 766625 lattice nodes, and it took 1.5 hrs to simulate 24 flapping cycles when run parallel in 8 cores.

As can be seen from figure 3, our predictions of the lift coefficient at a wing and the centre body matches well with the findings of Seo and Mittal (2011) and Wang et al. (2020). The current method also showed a good performance in capturing acoustic waves, see figure 4. In addition, the instantaneous flow field visualized by the vorticity field was similar to that of Seo and Mittal (2011), see figure 5. This validates numerical method presented in section 2 is suitable to examine fluid-structure-acoustic interaction problems.

4 Conclusions

An efficient and stable numerical method is developed to examine fluid-structure-acoustic interaction problems. The widely used immersed boundary lattice Boltzmann method is used to model the coupled fluid-structure system. To improve the stability of the numerical simulations, 4th order recursive and regularized BGK collision operator was implemented. The reflection of the sound waves into the fluid domain was minimized by applying the perfectly matched layer boundary condition. Two studies were performed with $2D$ and $3D$ solvers developed and found that the method performs well in handling moving boundaries and capturing acoustic waves. In future, this method will be used to examine acoustic generation by the flapping motion of flexible wings.

Acknowledgements

References

Brogi, F., Malaspinas, O., Chopard, B., and Bonadonna, C. (2017). Hermite regularization of the lattice Boltzmann method for open source computational aeroacoustics. *The Journal of the Acoustical Society of America*, 142(4):2332–2345.

Brogi, F., Ripepe, M., and Bonadonna, C. (2018). Lattice Boltzmann modeling to explain volcano acoustic source. *Scientific reports*, 8(1):1–8.

Cai, Y., Lu, J., and Li, S. (2018). Direct simulation of acoustic scattering problems involving fluid-structure interaction using an efficient immersed boundary-lattice Boltzmann method. *The Journal of the Acoustical Society of America*, 144(4):2256–2268.

Chen, L., Yu, Y., Lu, J., and Hou, G. (2014). A comparative study of lattice Boltzmann methods using bounce-back schemes and immersed boundary ones for flow acoustic problems. *International Journal for Numerical Methods in Fluids*, 74(6):439–467.

Coreixas, C., Wissocq, G., Puigt, G., Boussuge, J.-F., and Sagaut, P. (2017). Recursive regularization step for high-order lattice Boltzmann methods. *Physical Review E*, 96(3):033306.

Johnson, T. A. and Patel, V. C. (1999). Flow past a sphere up to a Reynolds number of 300. *Journal of Fluid Mechanics*, 378:19–70.

Kam, E., So, R., and Leung, R. (2007). Lattice Boltzman method simulation of aeroacoustics and nonreflecting boundary conditions. *AIAA journal*, 45(7):1703–1712.

Kang, S. K. and Hassan, Y. A. (2011). A comparative study of direct-forcing immersed boundary-lattice Boltzmann methods for stationary complex boundaries. *International Journal for Numerical Methods in Fluids*, 66(9):1132–1158.

Kim, J., Kim, D., and Choi, H. (2001). An immersed-boundary finite-volume method for simulations of flow in complex geometries. *Journal of Computational Physics*, 171(1):132–150.

Malaspinas, O. (2015). Increasing stability and accuracy of the lattice Boltzmann scheme: recursivity and regularization. *arXiv preprint arXiv:1505.06900*.

Najafi-Yazdi, A. and Mongeau, L. (2012). An absorbing boundary condition for the lattice Boltzmann method based on the perfectly matched layer. *Computers & fluids*, 68:203–218.

Poon, E. K. W., Ooi, A. S. H., Giacobello, M., Iaccarino, G., and Chung, D. (2014). Flow past a transversely rotating sphere at Reynolds numbers above the laminar regime. *Journal of Fluid Mechanics*, 759:751–781.

Rajamuni, R. D. M. M. (2018). *Flow-induced vibration of a spherical body*. PhD thesis, Monash University.

Roy, S., De, A., and Balaras, E. (2020). *Immersed Boundary Method*. Springer.

Seo, J. H. and Mittal, R. (2011). Computation of aerodynamic sound around complex stationary and moving bodies. In *49th AIAA Aerospace Sciences Meeting including the New Horizons Forum and Aerospace Exposition*, page 1087.

Shao, W. and Li, J. (2019). Review of lattice Boltzmann method applied to computational aeroacoustics. *Archives of Acoustics*, 44(2):215–238.

Sharma, K. V., Straka, R., and Tavares, F. W. (2020). Current status of lattice Boltzmann methods applied to aerodynamic, aeroacoustic, and thermal flows. *Progress in Aerospace Sciences*, 115:100616.

Tam, C. K. W. (2004). Computational aeroacoustics: An overview of computational challenges and applications. *International Journal of Computational Fluid Dynamics*, 18(6):547–567.

Wang, L., Tian, F. B., and Lai, J. (2020). An immersed boundary method for fluid–structure–acoustics interactions involving large deformations and complex geometries. *Journal of Fluids and Structures*, 95:102993.